Laser Fabrication of Large-Scale Nanoparticle Arrays for Sensing Applications

Arseniy I. Kuznetsov,*,† Andrey B. Evlyukhin,† Manuel R. Gonçalves,‡ Carsten Reinhardt,† Anastasia Koroleva,† Maria Luisa Arnedillo,† Roman Kiyan,† Othmar Marti,‡ and Boris N. Chichkov†

†Laser Zentrum Hannover e.V., Hollerithallee 8, 30419, Hannover, Germany, and ‡Institute of Experimental Physics, Ulm University, 89069, Ulm, Germany

ABSTRACT A novel method for high-speed fabrication of large scale periodic arrays of nanoparticles (diameters 40−200 nm) is developed. This method is based on a combination of nanosphere lithography and laser-induced transfer. Fabricated spherical nanoparticles are partially embedded into a polymer substrate. They are arranged into a hexagonal array and can be used for sensing applications. An optical sensor with the sensitivity of 365 nm/RIU and the figure of merit of 21.5 in the visible spectral range is demonstrated.

KEYWORDS: nanoparticle arrays · nanosphere lithography · LIFT · optical sensing

Development of biosensors based on localized surface plasmon resonance (LSPR) of metal nanoparticles attracted increasing attention during the past few years.[1−7] Compared to commercially available surface plasmon resonance (SPR) sensors[8] based on propagating surface plasmon modes in thin metal films, which have a typical probing depth of a few hundreds of nanometers, LSPR-based sensors allow measurements of refractive index changes in a close proximity to a metal nanoparticle in a near-field zone limited to a few tens of nanometers. This can make them suitable for detection of a single monolayer of biomolecules on their surface or even single molecule binding events on a single metal nanoparticle.[1,2,6] The main drawback of the existing LSPR sensors is their relatively low sensitivity, which is typically limited to a spectral resonance shift of a few hundreds of nanometers per refractive index unit (RIU). The overall performance of these sensors is characterized by their figure of merit (FOM), which is defined as a ratio of the sensitivity to the resonance peak width at the half-maximum.[9] The value of this parameter for LSPR-based sensors depends on the particle shape and size and typically does not exceed a few units owing to a high width of the plasmon resonance of a single nanoparticle.[10,11] Many recent studies were devoted to improvement of the figure of merit of the LSPR-based sensors using specially designed nanoparticle systems with narrow resonances.[12−19] These resonances appear due to near-field coupling of localized surface plasmons (LSP) of single nanoparticles and excitation of collective plasmon modes in the nanoparticle systems. These modes are localized inside the systems and can be applied for sensing similar to the LSPR of a single nanoparticle. Recent developments of this approach allowed experimental demonstration of an FOM value of 54 in the near-infrared spectral range.[20] Another possibility to realize a narrow resonance in the spectrum of a nanoparticle system is to use highly ordered nanoparticle arrays with diffractive (far-field) coupling of localized surface plasmons.[21−33] This approach was first discussed theoretically[21,22] and recently realized experimentally by several groups.[23−30] Similar systems but with an additional resonator layer under a nanoparticle array were also considered in earlier publications.[31,32] In a first study of sensing properties of such nanoparticle arrays using phase sensitive detection methods, very high sensitivity has been demonstrated.[33]

For sensing applications of nanoparticle structures and arrays, the main drawback is in high cost and low-throughput of existing fabrication methods. Most of the experimentally studied structures are fabricated by electron or ion beam lithographies, which are not suitable for large-scale production. This stimulates the development of new high-throughput and low-cost methods for the fabrication of nanoparticle structures with particular optical properties, for example, biosensors or metamaterials.[34,35]

In this paper, a novel method for high-speed fabrication of large-scale nanoparticle arrays is demonstrated. This method is based on a combination of nanosphere lithography and femtosecond laser-induced transfer.

* Address correspondence to a.kuznetsov@lzh.de.

Received for review March 9, 2011 and accepted May 3, 2011.

Published online May 03, 2011
10.1021/nn2009112

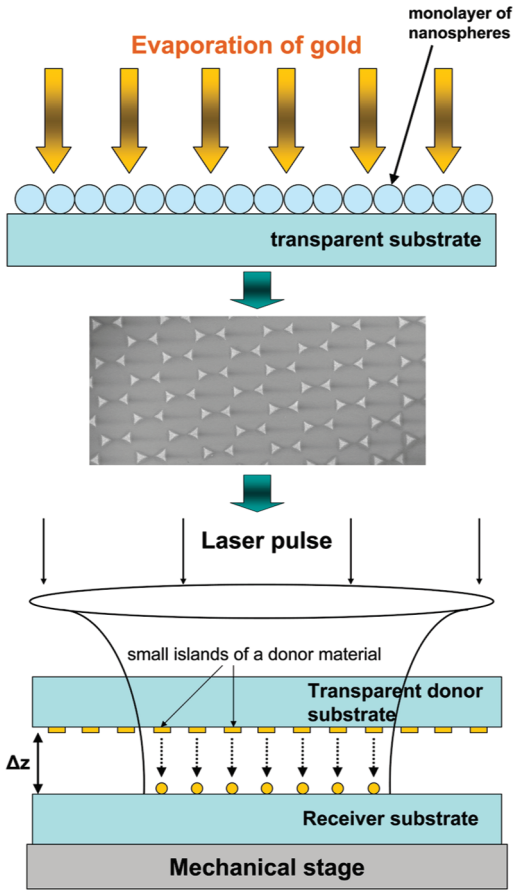

Figure 1. Scheme of nanoparticle structure fabrication by a combination of the nanosphere lithography and laser-induced transfer.

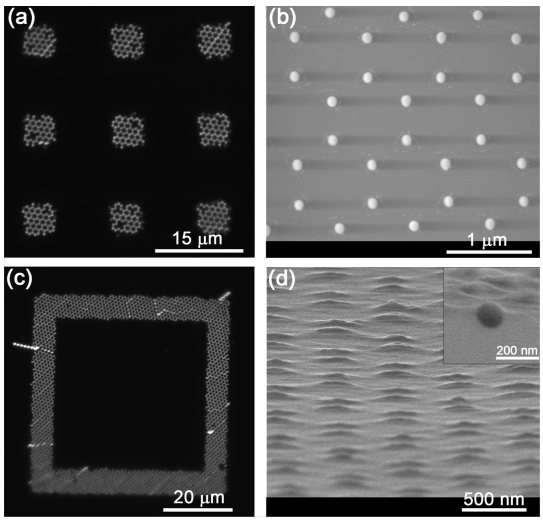

Figure 2. (a) Dark-field microscope image of arrays of gold nanoparticles fabricated by single laser pulses on a receiver substrate. Laser beam has a flat-top square-shaped profile with 6 μm size. Laser fluence is of 0.06 J/cm^2. (b) Top-view SEM image of a nanoparticle array fabricated by a single laser pulse. (c) Dark-field microscope image of a nanoparticle structure fabricated by multipulse laser irradiation at 1 kHz repetition rate and 1 mm/s sample translation speed. Laser beam profile and fluence are the same as in panel a. (d) Grazing incidence SEM image of a nanoparticle array fabricated at similar conditions as in panel c. Inset is a grazing incidence view of a nanoparticle located at the sample edge.

Fabricated structures consist of hexagonal arrays of spherical gold nanoparticles partially embedded into a polymeric substrate. Both interparticle distance and particle size can be independently controlled which allows engineering of optical properties of such arrays. In particular, it is shown that at some set of experimental parameters the transmission spectra of these nanoparticle arrays can possess very narrow dips with the full width at half-maximum (fwhm) down to 14 nm in the visible spectral range. These resonances appear due to diffractive coupling of localized surface plasmons of nanoparticles in these arrays. Their spectral position is very sensitive to the refractive index changes of local environment above the substrate with the nanoparticles. Finally, based on this novel fabrication method, cheap and easy-to-use sensors with a sensitivity of 350 nm/RIU and a figure of merit of 21.5 in the visible spectral range are demonstrated. Experimental results are supported by theoretical modeling based on the coupled dipole approach.

RESULTS AND DISCUSSION

A scheme of the novel method for high-speed fabrication of large-scale nanoparticle arrays based on a combination of the nanosphere lithography and laser-induced transfer is shown in Figure 1. A detailed description of this novel approach is given in the Methods section at the end of this paper.

Examples of gold nanoparticle structures fabricated on the receiver substrate by single femtosecond laser pulses are shown in Figure 2a,b. In this experiment, triangular donor structures were prepared using polystyrene spheres with 1 μm diameter and evaporation of 45 nm gold layer. The laser fluence of 0.06 J/cm^2 was used for the transfer process. As can be seen in the SEM images taken from different angles (top view is shown in Figure 2b, grazing incidence view is shown in the inset to Figure 2d), the transferred particles have spherical shape and they are arranged in a hexagonal array. The flat−top profile of the laser beam allows realizing the same irradiation conditions for each irradiated particle and transfer of many nanoparticles by a single laser pulse. On the other hand, by scanning the sample in horizontal directions any desired 2D structure consisting of nanoparticle arrays can be fabricated (Figure 2c). The arrangement of nanoparticles in a hexagonal array on the receiver substrate is independent of the laser beam profile or sample scanning direction and is completely determined by the original hexagonal structure on the donor substrate. The transferred nanoparticles are partially (about 70%) embedded into the soft receiver substrate as can be seen in the grazing incidence SEM image shown in Figure 2d. This makes these particles very

stable and resistant against cleaning and mechanical treatment of the sample.

Nanosphere lithography, which is applied for donor substrate preparation in this paper, is a cheap and simple approach for the fabrication of very large scale nanoparticle arrays. For this reason, nanosphere lithography is considered as very promising for different applications including biosensing.[1,2,4,36] One of the disadvantages of this method is a relatively low flexibility in controlling the size and shape of the fabricated triangular nanoparticles. The size of these triangles can be altered by changing the diameter of the nanospheres. However, this also changes the period of the hexagonal arrays. This, in particular, does not allow the realization of narrow resonances, due to diffractive coupling of localized surface plasmons, in optical spectra of such nanoparticle arrays.[21−30] To realize these narrow resonances, it is necessary to control independently the spectral position of the local plasmon resonance of nanoparticles (by varying the nanoparticle size) with respect to the diffractive resonance of the nanoparticle array (defined by the array period). This problem can be solved by melting the triangular prism nanostructures and their transformation into spherical nanoparticles. The size of these spherical nanoparticles depends not only on the triangle size but also on its thickness, which can be changed independently during the fabrication process. In previous studies, there were several attempts to realize such kind of transformation using thermal annealing[37−39] or laser-induced melting.[40,41] However, the thermal annealing of noble metal structures at high temperatures (600−900 °C for gold) results in the formation of hemispherical particles instead of spheres. On the other hand, liquid metallic spheres produced by nanosecond or femtosecond laser-induced melting are not stable on the substrate.[40,41] Indeed, fast transformation of a triangular metal prism into a liquid nanosphere initiates the center-of-mass movement in the upward direction normal to the substrate surface which is accompanied by acceleration, detachment, and jumping of the molten nanospheres.[40] Therefore, direct transformation of a triangular prism array into high quality nanosphere structure on the donor substrate surface is hardly possible.[37−41] By applying a laser-induced transfer method, as it is demonstrated in this paper, the desired transformation can be performed and highly ordered arrays of spherical nanoparticles can be produced. In this case, the jumping nanoparticles are simply caught on the receiver substrate. Conservation of the structural quality during the transfer process is achieved by a good contact between the donor and receiver substrates. It is also important that the transferred nanoparticles can be embedded into the receiver substrate, which makes them very stable and resistant against cleaning and mechanical treatments.

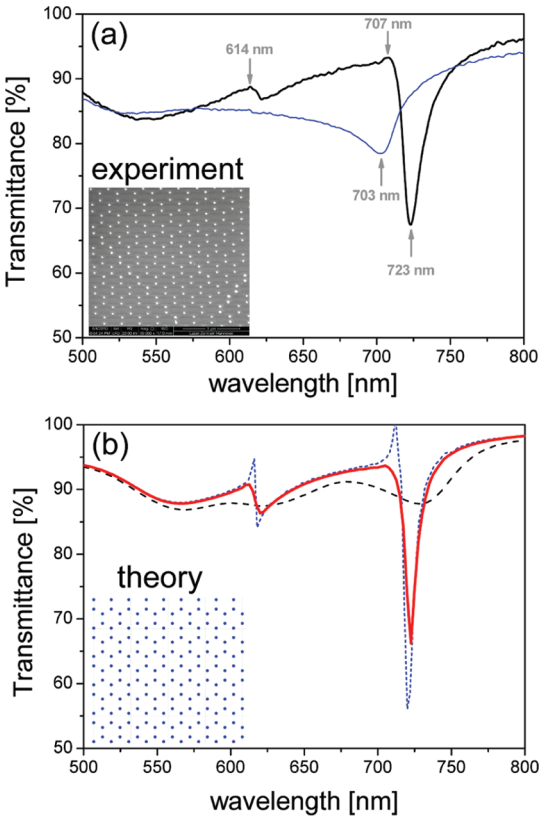

Figure 3. (a) Experimental transmission spectra of a hexagonal gold nanoparticle array partially embedded into a PDMS substrate in air (blue curve, inhomogeneous environment) and covered by a thick PDMS layer (black curve, homogeneous environment). The particle diameter is about 110 nm; the size of the unit cell is about 1100 nm (see Figure 2). Inset is a SEM image of the nanoparticle array taken at an angle of 45°. (b) Theoretical simulations of transmission spectra of a hexagonal nanoparticle array with the particle size of 108 nm and the unit cell size of 1132 nm placed in a homogeneous medium with the refractive index of 1.45 for the following sizes of the simulated structures: $5 \times 5\ \mu m^2$ (black dashed curve), $30 \times 30\ \mu m^2$ (red solid curve), and infinite (blue short dashed curve). These simulations were performed using a coupled dipole approach. Inset shows a scheme of the simulated structure.

Another important advantage of this method is that the size of the fabricated nanoparticles can be changed in a very wide range from a few hundreds of nanometers down to 10 nm. Indeed, commercially available nanospheres for nanosphere lithography have a minimum size of about 50 nm. The minimum thickness of good quality metal films, which can be achieved by thermal evaporation or other existing methods, is about 10 nm. This provides a theoretical limitation for the size of the fabricated spherical nanoparticles of about 10 nm, which is comparable to the size of nanoparticles produced by chemical methods in solutions. However, in contrast to chemical methods, laser-induced transfer allows fabrication of high-quality arrays of such nanoparticles. In our experiments, the smallest fabricated nanoparticle size was around 40 nm, which has been achieved using 400 nm

nanospheres and 20 nm gold coating. These nanoparticles are significantly smaller than that generated by laser-induced transfer of nanodroplets from homogeneous thin metal films (180 nm).[42−44] This is due to the small size of initial triangular structures, which are significantly smaller than the size of the focused laser beam irradiating a homogeneous film surface.

As it was mentioned above, both the interparticle distance and nanoparticle size in the transferred nanoparticle arrays can be independently controlled by changing the diameter of nanospheres and the thickness of evaporated material, respectively. This allows independent adjustment of both resonance positions (of the nanoparticle scattering and structural, diffractive resonance) and realization of special conditions when they are close to each another. The structural resonances are realized in the system at the wavelengths of Wood−Rayleigh's anomalies when one of the diffraction orders of the structure disappears inside the substrate.[27−29] When this wavelength is close to the wavelength of local plasmon resonance of nanoparticles, a collective plasmonic mode in the system can be excited. This corresponds to the diffractive coupling of localized surface plasmons of the nanoparticles.[27] An example of such resonant behavior in the hexagonal array of gold nanoparticles, fabricated by the laser-induced transfer, is shown in Figure 3a. The triangular donor structures for this array were prepared using 1 μm polystyrene spheres and 45 nm gold film evaporation. Laser-induced transfer was realized at the laser fluence of 0.06 J/cm^2, and sample translation speed of 1 mm/s. An array of gold nanoparticles of 1 $\times$ 1 mm^2 was fabricated in less than 4 min. Optical transmission measurements were carried out using a commercial fiber-equipped spectrometer (Ocean Optics, HR2000+). In Figure 3a, it can be seen that the transmission spectrum of the prepared sample has a broad dip at around 703 nm (blue curve). This dip corresponds to the excitation of a collective plasmonic mode in the nanoparticle system placed into inhomogeneous surroundings. It is known that narrow structural resonances can be realized in nanoparticle arrays embedded in a homogeneous medium, whereas for nanoparticles located on a substrate surface in air they disappear.[25] In our case, an intermediate situation is realized, since the transferred nanoparticles are partially embedded into the substrate. Note that nanoparticle arrays partially embedded into a substrate have been recently realized by more expensive methods including electron-beam lithography and reactive ion etching and demonstrated sharp collective plasmonic resonances.[30]

When an additional PDMS layer is placed on top of the nanoparticle array in order to realize a homogeneous environment around the nanoparticles, the structural resonance shifts to the red and becomes significantly narrower with the full width at half-maximum (fwhm) of only 14 nm (black curve in Figure 3a). This fwhm value of the structural resonance is close to the smallest values previously observed in nanoparticle systems prepared by electron-beam lithography[29] and corresponds to the resonance Q-factor of 52. This proves very good quality of the nanoparticle structures fabricated by the laser-induced transfer method. On the other hand, this experiment also shows that the spectral position of the resonance dip is sensitive to the refractive index of the local environment above the nanoparticle array, which makes this system very attractive for sensing applications.

To better understand the spectral behavior of these nanoparticle arrays, their optical response was analyzed theoretically using coupled-dipole equations.[45] Data for the dielectric function of gold were taken from Johnson and Christy.[46] Calculated transmission spectra of hexagonal gold nanoparticle arrays with different sizes placed in a homogeneous medium with the refractive index of 1.45 are shown in Figure 3b. The spherical nanoparticle diameter is 108 nm, and the unit cell size (the length of the longest diagonal in the hexagonal unit cell) is 1132 nm. These parameters provide the best correspondence to our experimental results. The calculated spectrum for the array with the size of 30 $\times$ 30 μm^2 (solid red curve) is very similar to the experimentally measured spectrum (black curve in Figure 3a). The size of 30 $\times$ 30 μm^2 corresponds to the typical size of defect-free areas on our sample. Defects in the samples appear due to imperfections of nanosphere monolayers during the donor preparation step. For smaller arrays, the resonance becomes less pronounced and almost disappears for the array with 5 $\times$ 5 μm^2 size (Figure 3b). On the other hand, an increase of the array size leads to further narrowing of the resonance. Calculations shown in Figure 3b demonstrate that further improvement of the colloidal crystal properties can lead to further increase of the structural resonance Q−factor.

To study sensing applications of the laser-fabricated nanoparticle arrays, a test solution of glycerin in water was added on top of the PDMS substrate containing nanoparticles. Transmission spectra of the nanoparticle array covered with solutions at different glycerin concentrations are shown in Figure 4a. The narrowest and most pronounced resonances are realized in the solutions with the refractive index close to 1.4, which is similar to the refractive index of PDMS. This corresponds to the case when the nanoparticles are embedded in a homogeneous medium. When the refractive index is lower or higher than that of the PDMS substrate, the resonance dip becomes broader and shifts to the blue or to the red spectral sides, correspondingly.

Spectral position dependence of the resonance dip on the refractive index of local environment (above the substrate with nanoparticles) is shown in Figure 4b. The sensor sensitivity, defined as a shift of the resonance

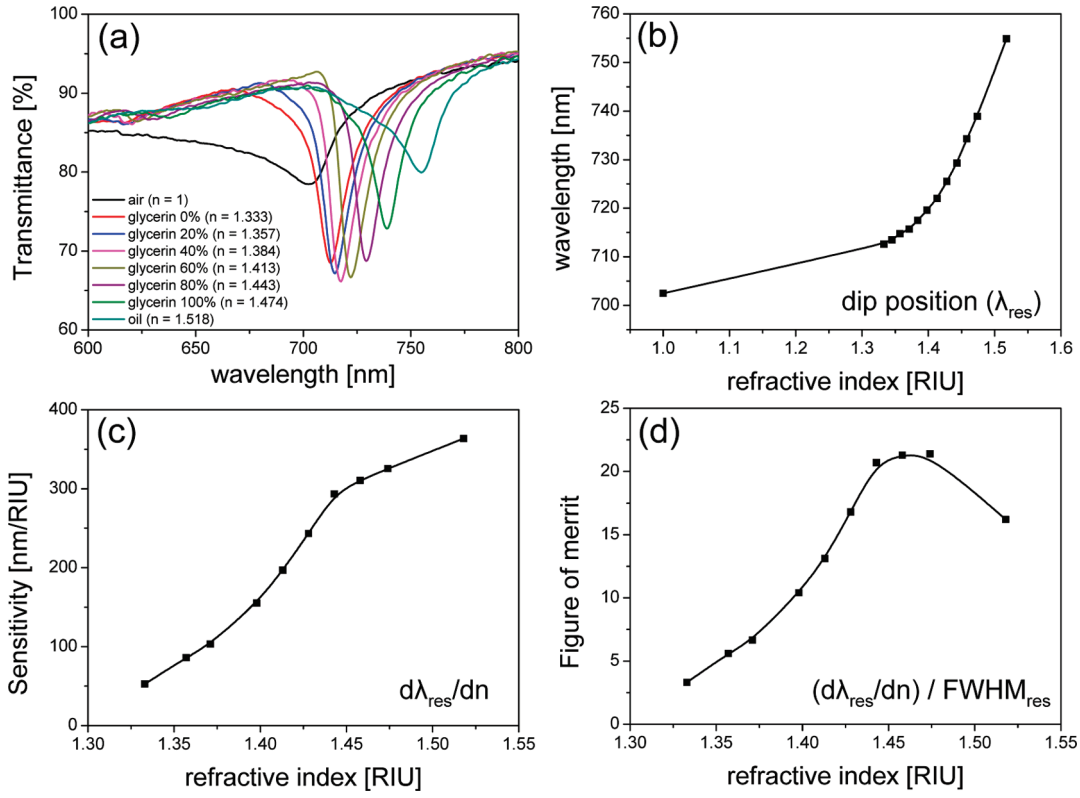

Figure 4. (a) Transmission spectra of the gold nanoparticle sensor array in different test solutions of glycerin in water. The content of glycerin in weight percents and corresponding refractive index of the solutions are shown in the panel. (b) Spectral position dependence of the resonance dips on the refractive index of the test solutions (*n*). (c) Dependence of the sensor sensitivity on the refractive index *n*. The sensitivity is calculated as a first derivative $d\lambda_{res}/dn$ of the dependence of the resonance position on *n* taken from panel b. (d) Figure of merit, calculated for each refractive index value as the sensitivity divided by the fwhm of the resonance dip. Black curves in panels b–d correspond to the B-Spline fit of experimental points (black squares).

wavelength induced by the change in the refractive index of the test medium, $d\lambda_{res}/dn$, is shown in Figure 4c for different values of *n*. As can be seen, the sensitivity monotonically grows with the refractive index and reaches its highest value of 365 nm/RIU in the case of immersion oil with the refractive index of 1.52. The obtained sensitivity values are typical for LSPR-based sensors.[1,2,10] The overall performance of the nanoparticle-based sensors is characterized by their figure of merit (FOM), which is defined as the ratio of their sensitivity to the resonance width at half-maximum.[9] Dependence of the figure of merit on the refractive index of local environment for our nanoparticle array sensor is shown in Figure 4d. One can see from this figure that the FOM grows with the refractive index of the tested medium (*n*) for $n < 1.47$ and then decreases. This happens due to the spectral broadening of the resonance dip when the refractive index of the local environment becomes higher than that of the substrate. The maximum FOM value of 21.5 is obtained for the refractive index of 1.47. This FOM value is among the highest experimentally obtained with nanostructure-based sensors.[19,20,34] It is also important that high FOM values are obtained in our case for solutions with the refractive index in the range of 1.33 to 1.5. This range corresponds to the typical refractive index values for most of biomaterials, which is important for biosensing applications.

Note that all results discussed in this paper were obtained with arrays of gold nanoparticles. In preliminary experiments, we have already tested that similar arrays can be fabricated with silver and silicon nanoparticles. In general, we expect that any material, which can be melted by laser irradiation, can be used for the fabrication of nanoparticle arrays by the method described in this paper. These highly ordered large-scale nanoparticle arrays can be also used for surface-enhanced Raman scattering (SERS)[1] and all-optical switching[47] applications.

CONCLUSION

A novel method for high-speed fabrication of large-scale periodic nanoparticle arrays has been developed. This method is based on a combination of nanosphere lithography with laser-induced transfer. First, large-scale hexagonal arrays of triangular prism structures are fabricated by the nanosphere lithography. Then these prisms are melted by femtosecond laser irradiation and transferred toward another (receiver) substrate. Millions of identical nanoparticles can be

transferred simultaneously by a single laser pulse. The transferred particles have spherical shape and are arranged into hexagonal arrays. They are partially embedded into the PDMS receiver substrate, which makes them stable and resistant against multiple cleaning and mechanical treatment procedures. Both the nanoparticle size and period of the nanoparticale array can be independently controlled in our experiment. In such nanoparticle arrays a collective plasmonic mode with diffractive coupling between the nanoparticles can be excited. Excitation of this mode leads to the appearance of a narrow (fwhm =14 nm) resonance dip in the optical transmission spectra. The spectral position of this dip is sensitive to the refractive index changes of the local environment which is promising for sensing applications. The sensitivity of 365 nm/RIU and the figure of merit (FOM) of 21.5 have been demonstrated in the visible spectral range using test water-glycerin solutions. This high sensing performance together with the fast and cheap fabrication procedure makes this nanoparticle array sensor promising for biomedical applications.

METHODS

Nanosphere Lithography. In our experiments, first, a hexagonal structure of gold triangles (triangular prisms) was fabricated on a glass (donor) substrate using nanosphere lithography (NL) (Figure 1). This method is based on the preparation of a lithographic mask consisting of an array of monodispersed colloidal spheres and physical vapor deposition of thin films over this mask.[48] After lift-off of the colloidal mask, a hexagonal array of plane triangular-shaped nanoparticles remains on the substrate surface. Colloidal spheres with different sizes from 400 nm to 3 μm, obeying the NIST standards, were purchased from Duke Scientific (now a division of Thermo Scientific). The colloidal polycrystal mask was prepared using crystallization induced by slow solvent evaporation from a nanosphere solution.[48] It permits the fabrication of sphere monolayers of up to 1 cm^2 area with many almost perfect monocrystals. A thin gold layer was thermally evaporated on top of the spheres at rates of 1 or 2 Å/s inside a vacuum chamber at 10^{-5}–10^{-6} mbar pressure.

Laser-Induced Transfer. Second, laser-induced transfer of the triangular structures from the donor onto a receiver substrate was realized, as schematically shown in Figure 1. In our experiments, we use a commercial 1 kHz femtosecond laser system (Tsunami+Spitfire, Spectra Physics) delivering 3 mJ, 30 fs laser pulses at a central wavelength of 800 nm. An image transfer scheme with 50× demagnification was realized in order to obtain a flat-top square-shaped laser beam profile on the sample surface.[49] Femtosecond laser pulses irradiate the back side of the donor substrate, as it is shown in Figure 1. The size of the laser beam is larger than the distance between the triangles in the hexagonal array which allows irradiating multiple triangular island structures by a single laser pulse. Another (receiver) substrate is placed in an ultimate contact with the donor sample ($\Delta z \rightarrow 0$). A good contact between the donor and receiver substrates is important to retain a good quality of the nanoparticle structures during the transfer process. In our experiments, it is realized using an elastic polymer polydimethylsiloxane (PDMS) substrate as a receiver. Triangular structures are melted by the laser irradiation and transformed into spherical droplets by strong surface tension forces. Droplets are ejected from the donor toward the receiver substrate due to inertia of the center-of-mass movement, which is initiated by surface tension-induced transformation of triangular prisms into spheres.[40] The ejected nanodroplets are attached to and partially embedded into the soft receiver substrate. The generated structures on both donor and receiver substrates are analyzed by scanning electron microscopy (SEM) and optical spectroscopy.

Acknowledgment. The authors acknowledge financial support for this work by the project CH179/20-1 and Schwerpunktprogramm SPP1391 "Ultrafast Nanooptics" of the Deutsche Forschungsgemeinschaft (DFG), the Centre of Excellence for Quantum Engineering and Space–Time Research (QUEST), and Project C10 of the SFB-569 (DFG). We thank M. Asbach for her contribution to the sample preparation and the Institute of Solid State Physics of the Ulm University for the thermal evaporation system.

REFERENCES AND NOTES

1. Anker, J. N.; Hall, W. P.; Lyandres, O.; Shah, N. C.; Zhao, J.; Van Duyne, R. P. Biosensing with Plasmonic Nanosensors. *Nat. Mater.* **2008**, *7*, 442–453.
2. Stuart, D. A.; Haes, A. J.; Yonzon, C. R.; Hicks, E. M.; Van Duyne, R. P. Biological Applications of Localised Surface Plasmonic Phenomenae. *IEE Proc. Nanobiotechnol.* **2005**, *152*, 13–32.
3. Jain, P. K.; Huang, X.; El-Sayed, I. H.; El-Sayed, M. A. Noble Metals on the Nanoscale: Optical and Photothermal Properties and Some Applications in Imaging, Sensing, Biology, and Medicine. *Acc. Chem. Res.* **2008**, *41*, 1578–1586.
4. Stewart, M. E.; Anderton, C. R.; Thompson, L. B.; Maria, J.; Gray, S. K.; Rogers, J. A.; Nuzzo, R. G. Nanostructured Plasmonic Sensors. *Chem. Rev.* **2008**, *108*, 494–521.
5. Sepúlveda, B.; Angelomé, P. C.; Lechuga, L. M.; Liz-Marzán, L. M. LSPR-Based Nanobiosensors. *Nano Today* **2009**, *4*, 244–251.
6. Mayer, K. M.; Hao, F.; Lee, S.; Nordlander, P.; Hafner, J. H. A Single Molecule Immunoassay by Localized Surface Plasmon Resonance. *Nanotechnology* **2010**, *21*, 255503.
7. Kabashin, A. V.; Evans, P.; Pastkovsky, S.; Hendren, W.; Wurtz, G. A.; Atkinson, R.; Pollard, R.; Podolskiy, V. A.; Zayats, A. V. Plasmonic Nanorod Metamaterials for Biosensing. *Nat. Mater.* **2009**, *8*, 867–871.
8. Homola, J.; Yee, S. S.; Gauglitz, G. Surface Plasmon Resonance Sensors: Review. *Sens. Actuators B* **1999**, *54*, 3–15.
9. Sherry, L. J.; Chang, S.–H.; Schatz, G. C.; Van Duyne, R. P.; Wiley, B. J.; Xia, Y. Localized Surface Plasmon Resonance Spectroscopy of Single Silver Nanocubes. *Nano Lett.* **2005**, *5*, 2034–2038.
10. Chen, H.; Kou, X.; Yang, Z.; Ni, W.; Wang, J. Shape- and Size-Dependent Refractive Index Sensitivity of Gold Nanoparticles. *Langmuir* **2008**, *24*, 5233–5237.
11. Liao, H.; Nehl, C. L.; Hafner, J. H. Biomedical Applications of Plasmon Resonant Metal Nanoparticles. *Nanomedicine* **2006**, *1*, 201–208.
12. Liu, N.; Weiss, T.; Mesch, M.; Langguth, L.; Eigenthaler, U.; Hirscher, M.; Sönnichsen, C.; Giessen, H. Planar Metamaterial Analogue of Electromagnetically Induced Transparency for Plasmonic Sensing. *Nano Lett.* **2010**, *10*, 1103–1107.
13. Hentschel, M.; Saliba, M.; Vogelgesang, R.; Giessen, H.; Alivisatos, A. P.; Liu, N. Transition from Isolated to Collective Modes in Plasmonic Oligomers. *Nano Lett.* **2010**, *10*, 2721–2726.
14. Liu, N.; Mesch, M.; Weiss, T.; Hentschel, M.; Giessen, H. Infrared Perfect Absorber and Its Application as Plasmonic Sensor. *Nano Lett.* **2010**, *10*, 2342–2348.

15. Stockman, M. I. Nanoscience: Dark–Hot Resonances. *Nature* **2010**, *467*, 541–542.
16. Lukyanchuk, B.; Zheludev, N. I.; Maier, S. A.; Halas, N. J.; Nordlander, P.; Giessen, H.; Chong, C. T. The Fano Resonance in Plasmonic Nanostructures and Metamaterials. *Nat. Mater.* **2010**, *9*, 707–715.
17. Lassiter, J. B.; Sobhani, H.; Fan, J. A.; Kundu, J.; Capasso, F.; Nordlander, P.; Halas, N. J. Fano Resonances in Plasmonic Nanoclusters: Geometrical and Chemical Tunability. *Nano Lett.* **2010**, *10*, 3184–3189.
18. Hao, F.; Sonnefraud, Y.; Van Dorpe, P.; Maier, S. A.; Halas, N. J.; Nordlander, P. Symmetry Breaking in Plasmonic Nanocavities: Subradiant LSPR Sensing and a Tunable Fano Resonance. *Nano Lett.* **2008**, *8*, 3983–3988.
19. Evlyukhin, A. B.; Bozhevolnyi, S. I.; Pors, A.; Nielsen, M. G.; Radko, I. P.; Willatzen, M.; Albrektsen, O. Detuned Electrical Dipoles for Plasmonic Sensing. *Nano Lett.* **2010**, *10*, 4571–4577.
20. Jeppesen, C.; Xiao, S.; Mortensen, N. A.; Kristensen, A. Metamaterial Localized Resonance Sensors: Prospects and Limitations. *Opt. Express* **2010**, *18*, 25075–25080.
21. Zou, S.; Janel, N.; Schatz, G. C. Silver Nanoparticle Array Structures That Produce Remarkably Narrow Plasmon Lineshapes. *J. Chem. Phys.* **2004**, *120*, 10871–10875.
22. Markel, V. A. Divergence of Dipole Sums and the Nature of Non-Lorentzian Exponentially Narrow Resonances in One-Dimensional Periodic Arrays of Nanospheres. *J. Phys. B* **2005**, *38*, L115–L121.
23. Hicks, E. M.; Zou, S.; Schatz, G. C.; Spears, K. G.; Van Duyne, R. P. Controlling Plasmon Line Shapes through Diffractive Coupling in Linear Arrays of Cylindrical Nanoparticles Fabricated by Electron Beam Lithography. *Nano Lett.* **2005**, *5*, 1065–1070.
24. Auguié, B.; Barnes, W. L. Collective Resonances in Gold Nanoparticle Arrays. *Phys. Rev. Lett.* **2008**, *101*, 143902.
25. Auguié, B.; Bendana, X. M.; Barnes, W. L.; García de Abajo, F. J. Diffractive Arrays of Gold Nanoparticles near an Interface: Critical Role of the Substrate. *Phys. Rev. B* **2010**, *82*, 155447.
26. Chu, Y.; Schonbrun, E.; Yang, T.; Crozier, K. B. Experimental Observation of Narrow Surface Plasmon Resonances in Gold Nanoparticle Arrays. *Appl. Phys. Lett.* **2008**, *93*, 181108.
27. Kravets, V. G.; Schedin, F.; Grigorenko, A. N. Extremely Narrow Plasmon Resonances Based on Diffraction Coupling of Localized Plasmons in Arrays of Metallic Nanoparticles. *Phys. Rev. Lett.* **2008**, *101*, 087403.
28. Vecchi, G.; Giannini, V.; Gómez Rivas, J. Shaping the Fluorescent Emission by Lattice Resonances in Plasmonic Crystals of Nanoantennas. *Phys. Rev. Lett.* **2009**, *102*, 146807.
29. Vecchi, G.; Giannini, V.; Gómez Rivas J. Surface Modes in Plasmonic Crystals Induced by Diffractive Coupling of Nanoantennas. *Phys. Rev. B* 2009, *80*, 201401(R).
30. Adato, R.; Yanik, A. A.; Wu, C.-H.; Shvets, G.; Altug, H. Radiative Engineering of Plasmon Lifetimes in Embedded Nanoantenna Arrays. *Opt. Express* **2010**, *18*, 4526–4537.
31. Linden, S.; Kuhl, J.; Giessen, H. Controlling the Interaction between Light and Gold Nanoparticles: Selective Suppression of Extinction. *Phys. Rev. Lett.* **2001**, *86*, 4688–4691.
32. Christ, A.; Zentgraf, T.; Kuhl, J.; Tikhodeev, S. G.; Gippius, N. A.; Giessen, H. Optical Properties of Planar Metallic Photonic Crystal Structures: Experiment and Theory. *Phys. Rev. B* **2004**, *70*, 125113.
33. Kravets, V. G.; Schedin, F.; Kabashin, A. V.; Grigorenko, A. N. Sensitivity of Collective Plasmon Modes of Gold Nanoresonators to Local Environment. *Opt. Lett.* **2010**, *35*, 956–958.
34. Henzie, J.; Lee, M. H.; Odom, T. W. Multiscale Pattering of Plasmonic Metamaterials. *Nat. Nanotechnol.* **2007**, *2*, 549–554.
35. Aksu, S.; Yanik, A. A.; Adato, R.; Artar, A.; Huang, M.; Altug, H. High-Throughput Nanofabrication of Infrared Plasmonic Nanoantenna Arrays for Vibrational Nanospectroscopy. *Nano Lett.* **2010**, *10*, 2511–2518.
36. Wang, X.; Summers, C. J.; Wang, Z. L. Large-Scale Hexagonal-Patterned Growth of Aligned ZnO Nanorods for Nano-optoelectronics and Nanosensor Arrays. *Nano Lett.* **2004**, *4*, 423–426.
37. Kempa, K.; Kimball, B.; Rybczynski, J.; Huang, Z. P.; Wu, P. F.; Steeves, D.; Sennett, M.; Giersig, M.; Rao, D.V.G.L.N.; Garnahan, D. L.; *et al.* Photonic Crystals Based on Periodic Arrays of Aligned Carbon Nanotubes. *Nano Lett.* **2003**, *3*, 13–18.
38. Zhang, G.; Wang, D.; Möhwald, H. Ordered Binary Arrays of Au Nanoparticles Derived from Colloidal Lithography. *Nano Lett.* **2007**, *1*, 127–132.
39. Haes, A. J.; Zou, S.; Schatz, G. C.; Van Duyne, R. P. A Nanoscale Optical Biosensor: The Long Range Distance Dependence of the Localized Surface Plasmon Resonance of Noble Metal Nanoparticles. *J. Phys. Chem. B* **2004**, *108*, 109–116.
40. Habenicht, A; Olapinski, M.; Burmeister, F.; Leiderer, P.; Boneberg, J. Jumping Nanodroplets. *Science* **2005**, *309*, 2043–2045.
41. Huang, W.; Qian, W.; El-Sayed, M. A. Photothermal Reshaping of Prismatic Au Nanoparticles in Periodic Monolayer Arrays by Femtosecond Laser Pulses. *J. Appl. Phys.* **2005**, *98*, 114301.
42. Kuznetsov, A. I.; Koch, J.; Chichkov, B. N. Laser-Induced Backward Transfer of Gold Nanodroplets. *Opt. Express* **2009**, *17*, 18820–18825.
43. Kuznetsov, A. I.; Evlyukhin, A. B.; Reinhardt, C.; Seidel, A.; Kiyan, R.; Cheng, W.; Ovsianikov, A.; Chichkov, B. N. Laser-Induced Transfer of Metallic Nanodroplets for Plasmonics and Metamaterial Applications. *J. Opt. Soc. Am. B* **2009**, *12*, B130–B138.
44. Kuznetsov, A. I.; Kiyan, R.; Chichkov, B. N. Laser Fabrication of 2D and 3D Metal Nanoparticle Structures and Arrays. *Opt. Express* **2010**, *18*, 21198–21203.
45. Evlyukhin, A. B.; Reinhardt, C.; Seidel, A.; Luk'yanchuk, B. S.; Chichkov, B. N. Optical Response Features of Si-Nanoparticle Arrays. *Phys. Rev. B* **2010**, *82*, 045404.
46. Johnson, P. B.; Christy, R. W. Optical Constants of the Noble Metals. *Phys. Rev. B* **1972**, *6*, 4370–4379.
47. Wurtz, G. A.; Pollard, R.; Hendren, W.; Wiederrecht, G. P.; Gosztola, D. J.; Podolskiy, V. A.; Zayats, A. V. Designed Ultrafast Optical Nonlinearity in a Plasmonic Nanorod Metamaterial Enhanced by Nonlocality. *Nat. Nanotechnol.* **2011**, *6*, 107–111.
48. Fischer, U.Ch.; Zingsheim, H. P. Submicroscopic Pattern Replication with Visible Light. *J. Vac. Sci. Technol.* **1981**, *19*, 881–885.
49. Kuznetsov, A. I.; Koch, J.; Chichkov, B. N. Nanostructuring of Thin Gold Films by Femtosecond Lasers. *Appl. Phys. A: Mater. Sci. Process.* **2009**, *94*, 221–230.